

# Timing and dynamics of Late Pleistocene mammal extinctions in southwestern Australia

Gavin J. Prideaux<sup>a,1</sup>, Grant A. Gully<sup>a</sup>, Aidan M. C. Couzens<sup>b</sup>, Linda K. Ayliffe<sup>c</sup>, Nathan R. Jankowski<sup>d</sup>, Zenobia Jacobs<sup>d</sup>, Richard G. Roberts<sup>d</sup>, John C. Hellstrom<sup>e</sup>, Michael K. Gagan<sup>c</sup>, and Lindsay M. Hatcher<sup>f</sup>

<sup>a</sup>School of Biological Sciences, Flinders University, Bedford Park, South Australia 5042, Australia; <sup>b</sup>School of Earth and Environment, University of Western Australia, Crawley, Western Australia 6009, Australia; <sup>c</sup>Research School of Earth Sciences, Australian National University, Canberra, Australian Capital Territory 0200, Australia; <sup>d</sup>Centre for Archaeological Science, School of Earth and Environmental Sciences, University of Wollongong, Wollongong, New South Wales 2522, Australia; <sup>e</sup>School of Earth Sciences, University of Melbourne, Melbourne, Victoria 3010, Australia; and <sup>f</sup>Augusta–Margaret River Tourism Association, Margaret River, Western Australia 6285, Australia

Edited by Paul L. Koch, University of California, Santa Cruz, CA, and accepted by the Editorial Board November 1, 2010 (received for review July 27, 2010)

**Explaining the Late Pleistocene demise of many of the world's larger terrestrial vertebrates is arguably the most enduring and debated topic in Quaternary science. Australia lost >90% of its larger species by around 40 thousand years (ka) ago, but the relative importance of human impacts and increased aridity remains unclear. Resolving the debate has been hampered by a lack of sites spanning the last glacial cycle. Here we report on an exceptional faunal succession from Tight Entrance Cave, southwestern Australia, which shows persistence of a diverse mammal community for at least 100 ka leading up to the earliest regional evidence of humans at 49 ka. Within 10 millennia, all larger mammals except the gray kangaroo and thylacine are lost from the regional record. Stable-isotope, charcoal, and small-mammal records reveal evidence of environmental change from 70 ka, but the extinctions occurred well in advance of the most extreme climatic phase. We conclude that the arrival of humans was probably decisive in the southwestern Australian extinctions, but that changes in climate and fire activity may have played facilitating roles. One-factor explanations for the Pleistocene extinctions in Australia are likely oversimplistic.**

climate change | human hunting | megafauna | fire history | paleoecology

Late Cenozoic vertebrate evolution is marked by the attainment of large body sizes within numerous lineages. Australian terrestrial environments were dominated by large marsupials, including giant wombats and short-faced kangaroos (1–3). Their radiation, which peaked during the Pleistocene, was the end-product of 15 million years of adaptation to increasingly drier conditions (3, 4). The disappearance, therefore, of most large species toward the close of the Pleistocene demands explanation, especially because records spanning the last five glacial–interglacial cycles show that central southern and southeastern Australian faunas were otherwise near-identical to their Holocene counterparts and resilient to climatic perturbations (4, 5). This finding has been used to bolster the view that the extinctions were human-caused (4, 5), but a lack of sites spanning the arid penultimate glacial maximum (PGM) has left open the possibility that many species succumbed during this period, leaving only a depauperate “megafauna” to greet humans 90 ka later (6).

Tight Entrance Cave (TEC) lies in the Leeuwin–Naturaliste Region (LNR), southwestern Australia (Fig. 1). The TEC fossil deposit was discovered and initially excavated by L.M.H. (1991–1995) and contains the richest and most diverse assemblage of Late Pleistocene vertebrates known from the western two-thirds of Australia (7). Excavations led by G.J.P. during 2007 to 2008 resulted in a refined understanding of the site and its chronology and a marked increase in samples over that reported upon for the earlier 1996 to 1999 excavation interval (7). Remains of 46 vertebrate and two gastropod species are recorded from TEC (Table 1). Mammals predominate in all units, and of the 40 species in total, 14 marsupials and one monotreme disappeared in the Late Pleistocene (Table 1). The giant snake *Wonambi naracoortensis* was lost during the same interval. Most animals were evidently pitfall vic-

tims, falling in alongside sediments and charcoal that were washed in via now-blocked solution pipes, although tooth marks on some bones suggest that the carnivores *Sarcophilus* and *Thylacoleo* played a minor accumulating role.

To establish an environmental background against which TEC faunal changes could be analyzed, we investigated stratigraphic variation in charcoal concentration, which reflects fire history (8), and stable-isotope ratios in aragonitic land-snail shells, a proxy for climate change. Taking these investigations into account with the local archeological record provides a unique single-locality dataset comprehensive enough to test the three dominant extinction hypotheses: human hunting, landscape burning, and increased aridity.

## Results and Discussion

**Chronology.** The chronology of the TEC faunal succession was established via uranium-series, optically stimulated luminescence and radiocarbon dating of samples excavated from a 21-m<sup>2</sup> by 1.8-m deep pit (Fig. 1C) within an 80-m<sup>2</sup> expanse of sandy sediments divisible into 10 units (Fig. 24). <sup>230</sup>Th/<sup>234</sup>U dating of an interbedded flowstone and optical dating of quartz grains provides ages for the oldest fossil-bearing layer (unit B) of 151 ± 7 and 135 ± 7 ka, respectively. Unit B is capped by a flowstone dated to 137 ± 2 ka (7). This unit is overlain within our excavation area by unit D, for which ages range from 119 ± 2 to 89 ± 6 ka. Ages for the remaining units are 70 ± 4 (unit E\*), 53 ± 4 to 43 ± 4 ka (units E–G), 37 ± 1 to 32 ± 3 ka (unit H), and 29.1 ± 0.2 ka (unit J). This dating makes TEC the only site on Earth known to have sampled a mammal community for 100 ka preceding regional human arrival and then subsequently.

**Environmental Records.** Bushfire history is reflected in the macrocharcoal (>200 μm) fraction, which records a local signal, and the microcharcoal (5–200 μm) fraction, which records predominantly regional-scale burning (8–10). The two charcoal size fractions are poorly correlated ( $R^2 = 0.244$ ), sharing less than 25% of the variation (*SI Appendix*). This finding is comparable to other stratigraphic charcoal studies (9) and supports the assumption of two charcoal provenances. Because solution pipes were narrow (<1.5 m diameter), little charcoal is likely to have entered the cave aerially, with most accumulating on the land surface as fallout from fires, before being washed in with sedi-

Author contributions: G.J.P., G.A.G., A.M.C.C., and L.K.A. designed research; G.J.P., G.A.G., A.M.C.C., L.K.A., N.R.J., Z.J., R.G.R., J.C.H., and L.M.H. performed research; G.J.P., G.A.G., A.M.C.C., L.K.A., N.R.J., Z.J., R.G.R., J.C.H., and M.K.G. analyzed data; and G.J.P., A.M.C.C., and L.K.A. wrote the paper.

The authors declare no conflict of interest.

This article is a PNAS Direct Submission. P.L.K. is a guest editor invited by the Editorial Board.

<sup>1</sup>To whom correspondence should be addressed. E-mail: gavin.prideaux@flinders.edu.au.

This article contains supporting information online at [www.pnas.org/lookup/suppl/doi:10.1073/pnas.1011073107/-DCSupplemental](http://www.pnas.org/lookup/suppl/doi:10.1073/pnas.1011073107/-DCSupplemental).

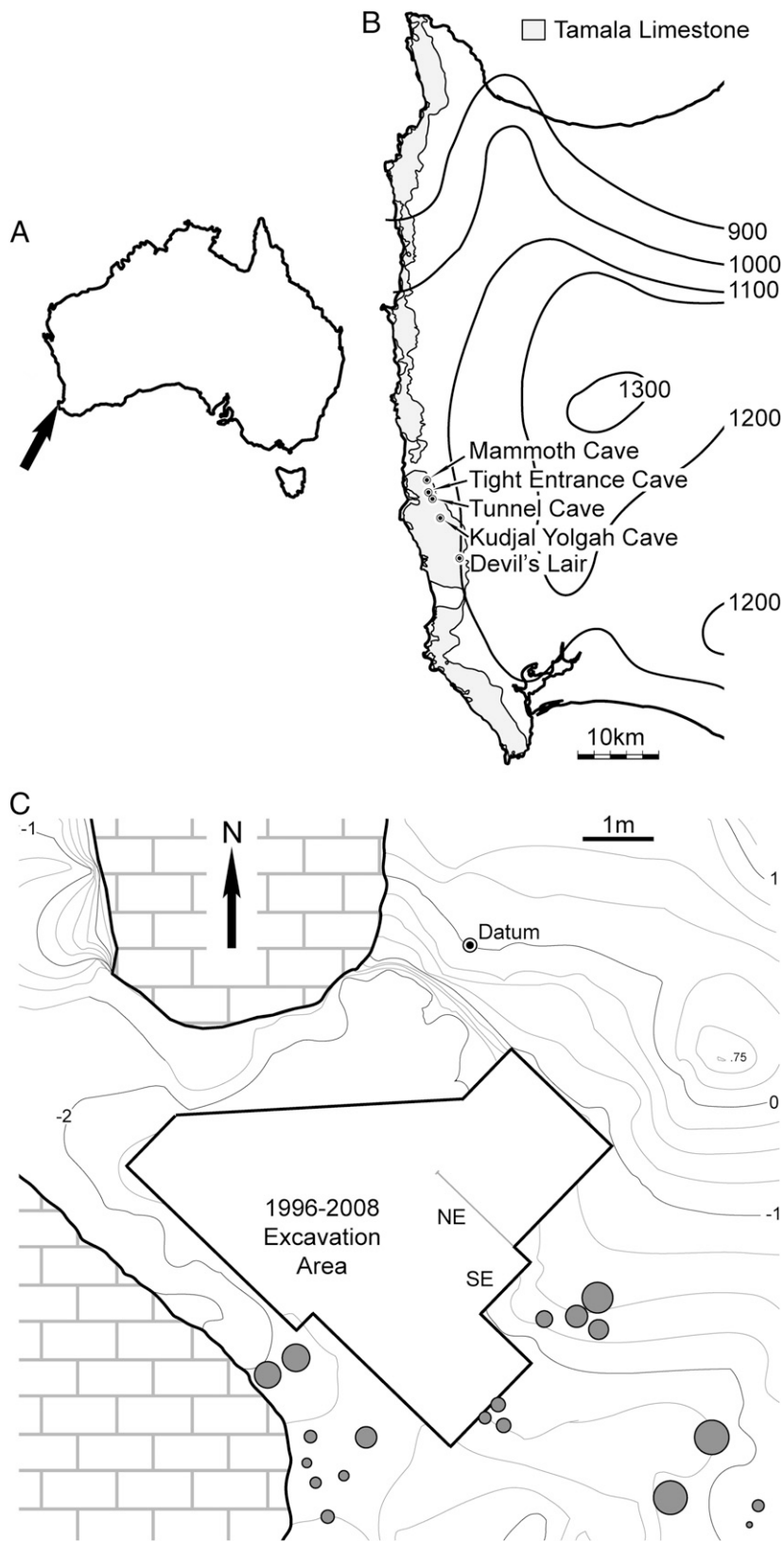


**Fig. 1.** Maps of southwestern Australia and Tight Entrance Cave. (A) Australia, with arrow indicating position of locality. (B) Leeuwin–Naturaliste Region, showing mean annual rainfall isohyets (mm), Tamala Limestone, and caves within it containing significant paleontological and archaeological deposits. (C) Plan view of main chamber showing excavation area. Stratigraphic sections (Fig. 2A) are denoted as NE and SE. Topographic heights (m) of sediment surface are measured relative to datum. Gray-filled circles denote stalagmites.

ments. Overall, both fractions show a major increase in unit E\* (70 ka), but the largest peaks occur near the top of the sequence in units H and J (37–29 ka) (Fig. 2B). The microcharcoal signal is particularly striking, with the mean concentration after 70 ka

( $96.5 \pm 59.4 \text{ mm}^2/\text{mL}$ ), more than four times higher than before ( $22.0 \pm 13.4 \text{ mm}^2/\text{mL}$ ), indicating a marked increase in regional fire activity. Removal of vegetation by burning increases sediment yield and runoff (11), and may explain significantly higher

**Table 1. Faunal list for the Tight Entrance Cave deposit**

Species	Body mass (kg)	Unit B 143	Unit D 104	Unit E* 70	Units E–G 48	Unit H 35	Unit J 31
<i>Tachyglossus aculeatus</i>	4.5		x				
<i>Thylacinus cynocephalus</i>	25	x	x	x	x	x	x
<i>Dasyurus geoffroii</i>	1.1	x	x	x	x	x	x
<i>Dasyercus cristicauda</i>	0.13		x				
<i>Sarcophilus harrisii</i>	9.0	x	x	x	x	x	x
<i>Antechinus flavipes</i>	0.04	x	x		x		
<i>Isoodon obesulus</i>	0.78	x	x		x	x	
<i>Perameles bougainville</i>	0.23	x	x	x	x		x
<i>Pseudocheirus occidentalis</i>	1.0		x		x	x	x
<i>Trichosurus vulpecula</i>	4.0	x	x	x	x	x	x
<i>Bettongia lesueur</i>	0.68		x		x	x	x
<i>Bettongia penicillata</i>	1.3	x	x	x			x
<i>Potorous gilbertii</i>	0.95	x	x	x	x	x	x
<i>Macropus fuliginosus</i>	49	x	x	x	x	x	x
<i>Macropus eugenii</i>	2.1		x				
<i>Macropus irma</i>	8.0	x	x	x	x	x	x
<i>Petrogale lateralis</i>	4.0				x		x
<i>Setonix brachyurus</i>	3.0	x	x	x	x	x	x
<i>Notomys</i> sp. indet.	0.05					x	x
<i>Pseudomys albocinerus</i>	0.03						x
<i>Pseudomys occidentalis</i>	0.03	x	x	x			
<i>Pseudomys shortridgei</i>	0.07		x				
<i>Rattus fuscipes</i>	0.14		x	x	x	x	x
<i>Megalibgwilia ramsayi</i> <sup>†</sup>	10		x				
<i>Phascolarctos cinereus</i> <sup>†</sup>	8.0	x	x	x			
<i>Vombatus hacketti</i> <sup>†</sup>	26	x	x	x	x		
Vombatidae sp. indet. <sup>†</sup>	300			x			
<i>Zygomaturus trilobus</i> <sup>†</sup>	500	x	x	x	x		
<i>Thylacoleo carnifex</i> <sup>†</sup>	104	x	x	x	x		
<i>Borongaboodie hatcheri</i> <sup>†</sup>	10		x				
<i>Congruus kitcheneri</i> <sup>†</sup>	40		x				
<i>Macropus</i> sp. nov. <sup>†</sup>	23	x	x	x			
<i>Protemnodon</i> sp. cf. <i>roechus</i> <sup>†</sup>	166	x	x	x	x		
<i>Sthenurus andersoni</i> <sup>†</sup>	72		x				
<i>Metasthenurus newtonae</i> <sup>†</sup>	55	x	x				
" <i>Procoptodon</i> " <i>browneorum</i> <sup>†</sup>	60	x	x	x	x	‡	
<i>Simosthenurus occidentalis</i> <sup>†</sup>	118	x	x	x	x	‡	
" <i>Simosthenurus</i> " <i>pales</i> <sup>†</sup>	150	x	x	x	x		

Mean ages (ka) are listed beneath unit name. See *SI Appendix* for derivation of body masses. *Phascogale calura* and *Sminthopsis crassicaudata* were collected from disturbed sediments; their precise stratigraphic provenance is unknown.

<sup>†</sup>Species became completely extinct in the Late Pleistocene, except for *Phascolarctos cinereus*, which became extinct locally only.

<sup>‡</sup>Remains reworked from underlying strata as evinced by preservation (*SI Appendix*, Fig. S4).

depositional rates after 70 ka, which are indicated by the greater thickness of post-70 ka sediments, relative to older beds accumulated over a longer interval (Fig. 24).

Variations in stable carbon and oxygen isotopes in snail shells reflect the isotopic contents of diet vegetation and ingested waters, as well as temperatures and relative humidities (12). We analyzed 31 *Bothriembryon sayi* shells from the TEC sequence and modern specimens from the land surface above. Serial samples were taken down their growth axes to assess seasonal changes in stable isotopes (*SI Appendix*). Grand mean  $\delta^{13}\text{C}$  values increase from unit D [ $-11.4 \pm 0.5$  (S.E.,  $1\sigma$ ) ‰;  $n = 6$ ] through unit J ( $-6.9 \pm 0.3\%$ ;  $n = 5$ ) (Fig. 3 and *SI Appendix*, Table S5). Grand mean  $\delta^{18}\text{O}$  values also show a progressive increase from unit B ( $-1.6 \pm 0.3\%$ ;  $n = 3$ ) to J ( $-0.6 \pm 0.2\%$ ;  $n = 5$ ) (Fig. 3). Increases in land-snail shell grand mean  $\delta^{13}\text{C}$  values (Fig. 3) and  $\delta^{13}\text{C}$  ranges (*SI Appendix*, Table S5) are consistent with changes from closed-canopy forests at around 100 ka to more open vegetation structures at around 30 ka. This consistency is because the  $\delta^{13}\text{C}$  values of  $\text{C}_3$  plants are sensitive to

water stress and light levels, increasing under conditions of greater water stress and decreasing under lower levels of irradiance. Although more difficult to interpret,  $\delta^{18}\text{O}_{\text{shell}}$  values support the conclusions drawn from  $\delta^{13}\text{C}_{\text{shell}}$  data. Should ice volume-corrected rainfall  $\delta^{18}\text{O}$  values have remained constant at this site over the past 150 ka, the  $\delta^{18}\text{O}_{\text{shell}}$  data suggests relative humidities and temperatures were declining, reaching a minimum at 33 to 29 ka (Fig. 3 and *SI Appendix*).

**Faunal Trends Through Time.** A broad size range of species characterizes all units (Table 1 and *SI Appendix*, Table S1), which implies that mechanisms of accumulation were consistent through the sequence. Therefore, changes in species relative abundances between units are likely to accurately reflect changes in the community prompted by environmental changes (5). Species richness is highest in unit D, mainly because of the greater number of smaller species (<5 kg body mass) (Fig. 44). However, by correcting for sample size using rarefaction analysis (*SI Appendix*),

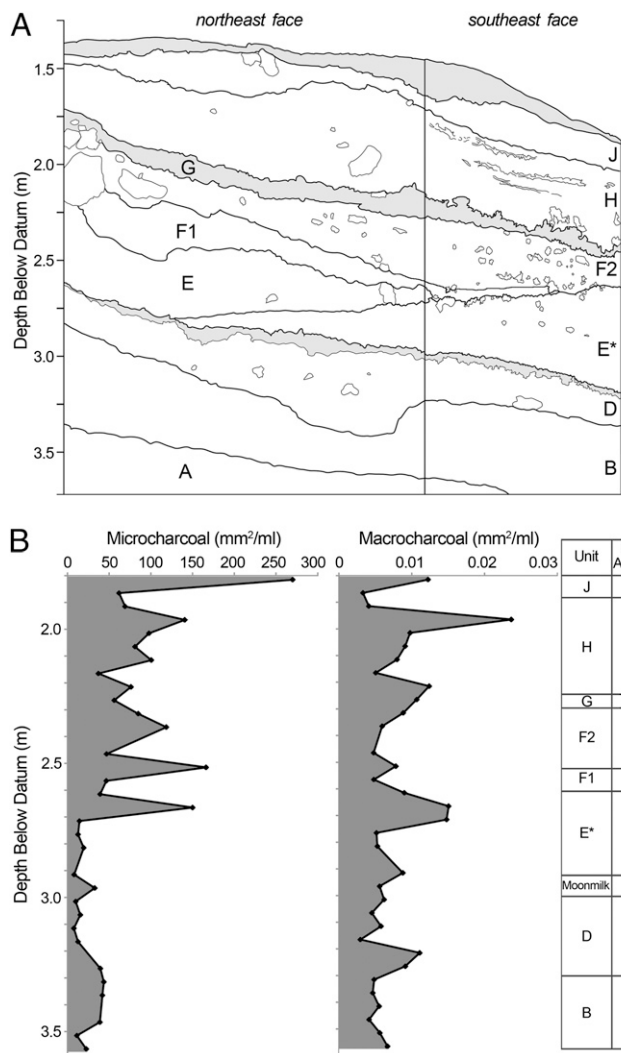


**Fig. 2.** Tight Entrance Cave stratigraphy and charcoal record. (A) Stratigraphic section with units (A–J) indicated. Units C and I were initially considered separate units but later identified as backfill layers from the initial Hatcher excavation (*SI Appendix*). Unit A is unfossiliferous. Shaded layers represent moonmilk (a fine crystalline limestone precipitate) spalled from the ceiling. (B) Stratigraphic trends in micro- and macrocharcoal collected from the southeast face of the excavation point to a distinct increase in regional fire activity from the time unit E\* accumulated ( $70 \pm 4$  ka).

we show that small mammal richness was fundamentally stable through time (Fig. 4A). Species richness of larger mammals (>5 kg) declines slightly from unit D through units E to G, but is halved from 12 to 6 species between units E to G and H. Among the 15 species lost in the Late Pleistocene, five have their last (or only) appearance in unit D, which records the most identified specimens (Table 1 and *SI Appendix*, Table S1). The five species not recorded beyond 89 ka are represented in unit D by only six specimens in total, so absence from younger units cannot necessarily be taken as evidence of absence from the fauna. Even unit E\* ( $70 \pm 4$  ka) contains a unique specimen of a distinct, unidentified wombat species (Table 1). In terms of sampling probability, it is unsurprising that, of the 15 imminently extinct species, the seven recorded in units E to G (53–43 ka) were among the most abundant species before 50 ka. None are represented in TEC units H and J (37–29 ka) by in situ remains (Table 1 and *SI Appendix*, Fig. S4).

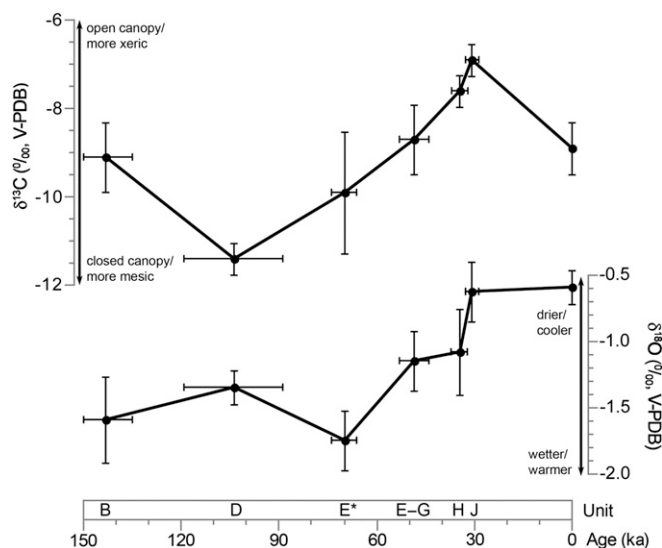


**Fig. 3.** Tight Entrance Cave stable-isotope record. Trends in stable carbon and oxygen isotopes from land-snail shells reveal declining relative humidities or temperatures following the accumulation of unit D (119–89 ka).  $\delta^{13}\text{C}$ ,  $\delta^{18}\text{O}$  values are expressed as mean  $\pm$  SE; horizontal bars denote errors on mean ages for units. Data have been corrected for ice volume contributions to  $\delta^{18}\text{O}$ , and changes in  $\delta^{13}\text{C}$  of atmospheric  $\text{CO}_2$  from fossil fuel burning (*SI Appendix*).

Relative species abundances from units B and D are remarkably similar (Fig. 4B–D), notwithstanding the extreme climates of the PGM [142–137 ka (13)] and last interglacial (about 125 ka), which occurred within the hiatus between the deposition of these units. Although we are thus unable to ascertain the degree of climatic impact on fauna during this interval, population recovery was evidently rapid. Land-snail stable-isotope values from unit D suggest a climate somewhat wetter than the present, in which a rainfall-controlled gradient prevails across the LNR between fire-sensitive, densely understoried karri forest in the south (mean annual rainfall 1,000–1,200 mm) and fire-promoting habitats characterized by jarrah, marri, *Agonis*, and *Banksia* species with a varied understorey in the north (rainfall 800–900 mm) (14). With the onset of the cooler conditions during which unit E\* (70 ka) accumulated, abundances for most species remain quite stable. Among the species that were to become extinct, only “*Procoptodon*” *browneorum* shows a substantial decline (Fig. 4B), a trend mirrored by the still-extant *Macropus fuliginosus* (Fig. 4C). Species including *Potorous gilbertii*, *Bettongia penicillata*, *Zygomaturus trilobus*, and *Thylacoleo carnifex* show increases (Fig. 4B and C). These shifts likely correlated with incipient reduction of forest and increased bushfire activity, as indicated by higher  $\delta^{13}\text{C}$  values and charcoal concentrations. Most species display minor or no shifts.

By the time unit H accumulated (37–32 ka), seven mammal species had disappeared from the record, including the last locally extant members of the Diprotodontidae, Thylacoleonidae, Vombatidae, and Sthenurinae. Two of these (“*P.*” *browneorum* and *Protemnodon roechus*) are represented by in situ remains dated to  $40 \pm 2$  ka in nearby Kudjal Yolghah Cave (Fig. 1 and *SI Appendix*, Fig. S5), but there are no younger records in the LNR. *Setonix brachyurus* declines steeply across this interval, and *Pseudocheirus occidentalis*, *P. gilbertii*, and *Rattus fuscipes* reach peak abundances in unit H (Fig. 4C). These changes reflect the spread of open sclerophyll vegetation, given the preference of *S. brachyurus* for dense undergrowth (15), *P. occidentalis* for the favorable nesting trees characteristic of these habitats (15), and *P. gilbertii* and *R. fuscipes* [by analogy with eastern Australian

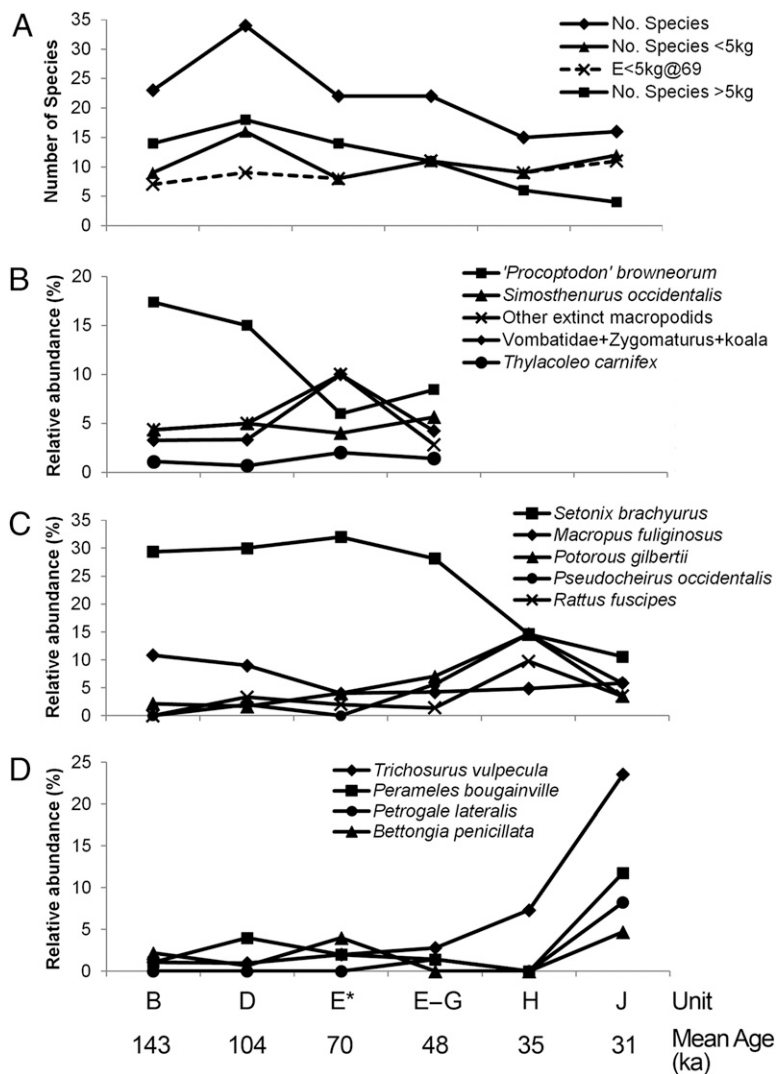


**Fig. 4.** Species richness and relative abundance trends through Tight Entrance Cave sequence. (A) Species richness for all mammals, and for small (<5 kg) and large (>5 kg) species. Expected small mammal species richness (E) is derived from rarefaction analysis (SI Appendix). (B) Relative abundance trends of larger taxa that have their last appearance in units E to G (53–43 ka) reveal evidence of an overall decline in only one species, “P.” *browneorum*. (C) Relative abundance trends for a range of smaller species point to a change in environmental conditions after 44 ka. *S. brachyurus* shows a marked decline, whereas *P. gilbertii*, *P. occidentalis*, and *R. fuscipes* increase, a likely response to spreading open sclerophyll vegetation. (D) Open-woodland species sharply increase in abundance in unit J (31 ka) in the lead-up to the LGM.

counterparts (16)] for mosaic understories. These shifts may reflect responses to the cumulative impact of climate change from 70 ka and intensification of aridity from around 40 ka, as echoed in a pollen record off the central Western Australian coast (17). Opening of vegetation in the lead-up to the last glacial maximum (LGM) is indicated by the abundances in unit J of species that prefer dry, open woodlands (e.g., *Petrogale lateralis*, *Perameles bougainville*, *B. penicillata*, *Trichosurus vulpecula*) (Fig. 4D). These faunal trends are reversed after the LGM, with species favored by the returning denser vegetation increasing in abundance (14).

### Conclusions

By demonstrating that the extreme climate of the PGM had no lasting impact on the LNR fauna, we counter the notion (6) that it triggered the demise of many larger taxa. This finding is consistent with records from southeastern Australia that show long-term resilience of mammal species until well into the last glacial (5, 18). Although it is clear that the loss of a diverse range of larger species between 50 and 40 ka occurred during a drying phase, the extinctions preceded the marked increase in aridity leading into the LGM. In light of this evidence, the long-term record, and the survival of all other mammals to modern times, the extinctions cannot solely or primarily have been the result of climate change.

The earliest evidence for humans in the LNR dates to  $49 \pm 2$  ka (19, 20); the youngest dated local remains of an extinct mammal species is  $40 \pm 2$  ka. This finding suggests at least several millennia of overlap, particularly in view of the Signor–Lipps effect (21). That is, it is highly improbable that the Devil’s Lair record (19) captures the first foray of humans into the region and that Kudjal Yolgha Cave contains the remains of the last-surviving individuals of all larger mammal species (except for the western gray kangaroo and thylacine). This rules out a classic “blitzkrieg” scenario (22, 23) as a viable explanation for the extinctions.

Landscape firing by humans may have played a role; people historically used fire to modify LNR vegetation (14) and the TEC record suggests greater bushfire activity in the lead-up to the LGM than in the equivalent climatic phase 100 ka earlier (Fig. 2B). However, the first spikes in regional fire activity occurred 20 ka before both the extinctions and the earliest indications of human occupation. This pattern contrasts with evidence for the role of human-lit fires in the extinction of a giant flightless bird in central Australia at 50 ka (24). On balance, human impacts (e.g., hunting, habitat alteration) were most likely the primary driver of the extinctions, but it is equally probable that the ultimate extinction “cause” was complex, and that landscape burning and increasing aridity helped fuel the extinction process. This study, therefore, provides empirical evidence for the interplay of different factors in the extinctions, which suggests that one-factor

explanations for the Australian Pleistocene extinctions are likely over-simplistic.

## Materials and Methods

**Paleontology.** The excavation area was divided into a series of variably sized grids, with excavation proceeding according to unit using standard paleontological methods. Depths of unit boundaries were measured relative to a datum point established within an adjacent limestone slab. Excavated sediment was sieved and resultant residues of small vertebrate remains then dried and sorted (picked) for taxonomically identifiable remains. Larger bones were cleaned, dried, and stabilized with polyvinyl butyrate dissolved in acetone. Specimens are deposited in the Department of Earth and Planetary Sciences, Western Australian Museum, Perth. Paleocological methods are outlined in the *SI Appendix*. Numbers of identifiable specimens for each species were recorded in spreadsheets according to grid, level, and unit. From this, the minimum numbers of individuals (MNI) for each species within stratigraphic units was calculated (*SI Appendix, Table S1*). It is an estimate of the lowest number of animals that would account for all identified specimens of a species. Here, it is a measure of the most abundant of four elements: left or right maxillary specimen or left or right dentary specimen. Relative abundance (MNIspecies/MNItotal%) is the most widely used measure of species incidence.

**Geochronology.**  $^{230}\text{Th}/^{234}\text{U}$  dating was conducted on solid pieces of calcite of  $\approx 30$  mg, cut from the speleothem samples using a dental drill. Samples were dissolved in nitric acid and equilibrated with a mixed  $^{229}\text{Th}$ – $^{233}\text{U}$  tracer. U and Th were extracted using Eichrom TRU resin before introduction to a Nu Plasma MC-ICP-MS, where isotope ratios of both elements were measured simultaneously (25). A well-constrained initial  $^{230}\text{Th}/^{232}\text{Th}$  activity ratio of  $0.245 \pm 0.035$  was determined and its uncertainty fully propagated (26). Optical dating provides an estimate of time elapsed since luminescent minerals, such as quartz, were last exposed to sunlight (2, 27). In this study, the event being dated is the time of entry of sediment grains into the caves. Optical ages for buried quartz grains were calculated from the burial dose (estimated using the optically stimulated luminescence signal) divided by the

dose rate from ionizing radiation. Bones sampled contained insufficient collagen for direct  $^{14}\text{C}$  dating, but charcoal clasts have been dated previously (7). Errors on all ages are reported at  $1\sigma$ .

**Charcoal Analysis.** Sediment samples were collected in continuous 5-cm increments and each sample spiked with a *Lycopodium* tablet ( $n = 12,542$ , batch 124,961), carbonates removed with 5% HCl and silicates removed with a HF acid treatment. Samples were deflocculated with hot 10% NaOH, treated with 4-min acetolysis to remove organics, and then washed through 200- and 5- $\mu\text{m}$  screens. Macrocharcoal ( $>200 \mu\text{m}$ ) grain diameter and frequency were determined under a low-power optical microscope using a grid-square technique and the square of geometric mean diameter used to estimate macrocharcoal concentration (28). Using a minimum grain count of 200, point counts of eurette slide preparations were used to estimate microcharcoal (5–200  $\mu\text{m}$ ) concentration (29).

**Stable Isotope Analysis.** Land-snail tests were treated with 3%  $\text{H}_2\text{O}_2$  to remove organic compounds before sectioning with a small diamond-impregnated grinding wheel (*SI Appendix*). Powdered samples of land-snail shell aragonite ( $\sim 200 \mu\text{g}$ ) were reacted at  $90^\circ\text{C}$  in a Kiel carbonate device and analyzed on a Finnigan MAT251 mass spectrometer. Isotope results were standardized to the V-Pee Dee Belemnite scale by in-run comparison with NBS-19 and NBS-18.  $\delta^{13}\text{C}$ ,  $\delta^{18}\text{O}$  ‰ =  $[(R_{\text{sample}}/R_{\text{standard}}) - 1] \times 1,000$ , where R is the  $^{13}\text{C}/^{12}\text{C}$  or  $^{18}\text{O}/^{16}\text{O}$  ratio. Reproducibility of  $\delta^{13}\text{C}$  and  $\delta^{18}\text{O}$  for NBS-19 ( $n = 80$ ) during the period of analysis was  $\pm 0.02\text{‰}$  and  $\pm 0.03\text{‰}$  (both at  $1\sigma$ ), respectively.

**ACKNOWLEDGMENTS.** We thank the many volunteers, students, colleagues, and friends for assistance with excavations over the past 14 years, particularly Anthony O’Flaherty for surveying. Pia Atahan, Bill Wilson, and Lorraine Wilson assisted with charcoal analysis. Funding and logistic support was provided by the Australian Research Council, Western Australian Department of Environment and Conservation, the Augusta–Margaret River Tourism Association, and the Western Australian Museum.

1. Koch PL, Barnosky AD (2006) Late Quaternary extinctions: State of the debate. *Annu Rev Ecol Syst* 37:215–250.
2. Roberts RG, et al. (2001) New ages for the last Australian megafauna: Continent-wide extinction about 46,000 years ago. *Science* 292:1888–1892.
3. Prideaux GJ (2004) *Systematics and Evolution of the Sthenurine Kangaroos* (Univ Calif Publ Geol Sci, Berkeley), Vol. 146.
4. Prideaux GJ, et al. (2007) An arid-adapted middle Pleistocene vertebrate fauna from south-central Australia. *Nature* 445:422–425.
5. Prideaux GJ, et al. (2007) Mammalian responses to Pleistocene climate change in southeastern Australia. *Geology* 35:33–36.
6. Wroe S, Field JH (2006) A review of the evidence for a human role in the extinction of Australian megafauna and an alternative interpretation. *Quat Sci Rev* 25:2692–2703.
7. Ayliffe LK, et al. (2008) Age constraints on Pleistocene megafauna at Tight Entrance Cave in southwestern Australia. *Quat Sci Rev* 27:1784–1788.
8. Whitlock C, Millspaugh SH (1996) Testing the assumptions of fire history studies: An examination of modern charcoal accumulation in Yellowstone National Park, USA. *Holocene* 6:7–15.
9. Carcaillet C, et al. (2001) Comparison of pollen-slide and sieving methods in lacustrine charcoal analyses for local and regional fire history. *Holocene* 11:467–476.
10. Lynch JA, Clark JS, Stocks BJ (2004) Charcoal production, dispersal and deposition from the Fort Providence experimental fire: Interpreting fire regimes from charcoal records in boreal forests. *Can J For Res* 34:16–42.
11. Shakesby RA, Doerr SH (2006) Wildfire as a hydrological and geomorphological agent. *Earth-Sci Rev* 74:269–307.
12. Balakrishnan M, Yapp CJ (2004) Flux balance model for the oxygen and carbon isotope composition of land snail shells. *Geochim Cosmochim Acta* 68:2007–2024.
13. Thomas AL, et al. (2009) Penultimate deglacial sea-level timing from uranium/thorium dating of Tahitian corals. *Science* 324:1186–1189.
14. Dortch J (2004) Late Quaternary vegetation change and the extinction of Black-flanked rock-wallaby (*Petrogale lateralis*) at Tunnel Cave, southwestern Australia. *Palaeogeogr Palaeoclimatol Palaeoecol* 211:185–204.
15. van Dyck S, Strahan R (2008) *Mammals of Australia* (Reed New Holland, Sydney), 3rd Ed.
16. Bennet AF (1993) Microhabitat use by the long-nosed potoroo, *Potorous tridactylus*, and other small mammals in remnant forest vegetation, south-western Victoria. *Wildl Res* 20:267–285.
17. van der Kaars S, De Deckker P (2002) A Late Quaternary pollen record from deep-sea core Fr10/95, GC17 offshore Cape Range Peninsula, northwestern Western Australia. *Rev Palaeobot Palynol* 120:17–39.
18. Macken AC (2009) A palaeoecological investigation of the Grant Hall fossil deposit, Victoria Fossil Cave, Naracoorte, South Australia. B.Sc.(Hons) Thesis, (Flinders University, Adelaide, Australia).
19. Turney CSM, et al. (2001) Early human occupation at Devil’s Lair, southwestern Australia 50,000 years ago. *Quat Res* 55:3–13.
20. Reimer PJ, et al. (2009) IntCal09 and Marine09 radiocarbon age calibration curves, 0–50000 years cal BP. *Radiocarbon* 51:1111–1150.
21. Signor PW, Lipps JH (1982) Sampling bias, gradual extinction patterns and catastrophes in the fossil record. *Spec Pap Geol Soc Am* 190:291–296.
22. Brook BW, Bowman DMJS (2004) The uncertain blitzkrieg of Pleistocene megafauna. *J Biogeogr* 31:517–523.
23. Gillespie R, Brook BW, Baynes A (2006) Short overlap of people and megafauna in Pleistocene Australia. *Alcheringa Spec Iss* 1:163–185.
24. Miller GH, et al. (2005) Ecosystem collapse in Pleistocene Australia and a human role in megafaunal extinction. *Science* 309:287–290.
25. Hellstrom JC (2003) Rapid and accurate U/Th dating using parallel ion-counting multicollector ICP-MS. *J Anal At Spectrom* 18:1346–1351.
26. Hellstrom JC (2006) U–Th dating of speleothems with high initial  $^{230}\text{Th}$  using stratigraphical constraint. *Quat Geochron* 1:289–295.
27. Jacobs Z, Roberts RG (2007) Advances in optically stimulated luminescence dating of individual grains of quartz from archeological deposits. *Evol Anthropol* 16:210–223.
28. Clark JS, Hussey TC (1996) Estimating the mass flux of charcoal from sediment records: The effect of particle size, morphology, and orientation. *Holocene* 8:129–144.
29. Clark RL (1982) Point count estimation of charcoal in pollen preparations and thin-sections of sediments. *Pollen et Spores* 24:523–535.